PNAS RESEARCH ARTICLE | MICROBIOLOGY OPEN ACCESS

Maladaptation after a virus host switch leads to increased activation of the pro-inflammatory NF-κB pathway

Huibin Yu[a], Chen Peng[b], Chi Zhang[a], Ana M. M. Stoian[a], Loubna Tazi[a], Greg Brennan[a], and Stefan Rothenburg[a,1]

Edited by Harmit Malik, Fred Hutchinson Cancer Research Center, Seattle, WA; received August 19, 2021; accepted March 18, 2022

Myxoma virus (MYXV) causes localized cutaneous fibromas in its natural hosts, tapeti and brush rabbits; however, in the European rabbit, MYXV causes the lethal disease myxomatosis. Currently, the molecular mechanisms underlying this increased virulence after cross-species transmission are poorly understood. In this study, we investigated the interaction between MYXV M156 and the host protein kinase R (PKR) to determine their crosstalk with the proinflammatory nuclear factor kappa B (NF-κB) pathway. Our results demonstrated that MYXV M156 inhibits brush rabbit PKR (bPKR) more strongly than European rabbit PKR (ePKR). This moderate ePKR inhibition could be improved by hyperactive M156 mutants. We hypothesized that the moderate inhibition of ePKR by M156 might incompletely suppress the signal transduction pathways modulated by PKR, such as the NF-κB pathway. Therefore, we analyzed NF-κB pathway activation with a luciferase-based promoter assay. The moderate inhibition of ePKR resulted in significantly higher NF-κB–dependent reporter activity than complete inhibition of bPKR. We also found a stronger induction of the NF-κB target genes TNFα and IL-6 in ePKR-expressing cells than in bPKR-expressing cells in response to M156 in both transfection and infections assays. Furthermore, a hyperactive M156 mutant did not cause ePKR-dependent NF-κB activation. These observations indicate that M156 is maladapted for ePKR inhibition, only incompletely blocking translation in these hosts, resulting in preferential depletion of short–half-life proteins, such as the NF-κB inhibitor IκBα. We speculate that this functional activation of NF-κB induced by the intermediate inhibition of ePKR by M156 may contribute to the increased virulence of MYXV in European rabbits.

poxvirus | myxoma virus | PKR | eIF2 | NF-κB

Significance

Myxoma virus (MYXV) is benign in the natural brush rabbit host but causes a fatal disease in European rabbits. Here, we demonstrate that MYXV M156 inhibited brush rabbit protein kinase R (bPKR) more efficiently than European rabbit PKR (ePKR). Because ePKR was not completely inhibited by M156, there was a depletion of short–half-life proteins like the nuclear factor kappa B (NF-κB) inhibitor IκBα, concomitant NF-κB activation and NF-κB target protein expression in ePKR-expressing cells. NF-κB pathway activation was blocked by either hypoactive or hyperactive M156 mutants. This demonstrates that maladaptation of viral immune antagonists can result in substantially different immune responses in aberrant hosts. These different host responses may contribute to altered viral dissemination and may influence viral pathogenesis.

The ongoing severe acute respiratory syndrome coronavirus 2 (SARS–CoV-2) pandemic highlights the risk of cross-species transmission events in the modern world. SARS–CoV-2 and other emerging viruses such as monkeypox virus, Middle East respiratory syndrome coronavirus, and Ebola virus appear to cause enhanced morbidity and mortality in their new hosts compared to their natural hosts. This increased virulence is not a universal feature of cross-species transmission, and the molecular and evolutionary determinants of differential virulence in new hosts are poorly understood (1). Furthermore, defining the determinants of different host responses is often difficult either because the natural host is unknown or little is known about the virulence of a pathogen in the reservoir species. However, one of the best-known examples of this increased virulence after cross-species transmission is the lagomorph-specific poxvirus, myxoma virus (MYXV).

MYXV naturally circulates in the South and Central American tapeti (forest rabbit, *Sylvilagus brasiliensis*) and the North American brush rabbit (*Sylvilagus bachmani*). In these host species, MYXV usually causes innocuous cutaneous fibroma (2). However, when European rabbits (*Oryctolagus cuniculus*) are infected, it causes the highly lethal disseminated disease myxomatosis (3). Symptoms of acute myxomatosis are characterized by an abnormal inflammatory response including fever, edema, mucopurulent conjunctivitis, and rhinitis (4). In the 1950s, an attempt to reduce the invasive European rabbit population in Australia was undertaken by releasing this extremely pathogenic virus into the wild (5). Not long after this intentional release, attenuated strains of MYXV began to emerge in wild populations, reducing the case fatality rate from 99.8% to 50 to 70% in Australian rabbits (6, 7). We previously characterized a naturally occurring mutation in the MYXV protein kinase R (PKR) inhibitor M156, L98P, that abrogated the ability of M156 to inhibit rabbit PKR and led to MYXV attenuation in cultured cells (8). These data indicate that the PKR pathway might contribute to the severe pathogenicity of MYXV in European rabbits.

Double-stranded (ds) RNA–dependent PKR is an interferon-stimulated host immune protein that is activated by dsRNA generated during viral replication (9, 10). Activated

Author contributions: H.Y., C.P., L.T., G.B., and S.R. designed research; H.Y., C.P., C.Z., A.M.M.S., L.T., and S.R. performed research; H.Y., C.P., and S.R. contributed new reagents/analytic tools; H.Y., C.P., C.Z., A.M.M.S., L.T., G.B., and S.R. analyzed data; and H.Y., G.B., and S.R. wrote the paper.

The authors declare no competing interest.

This article is a PNAS Direct Submission.

[1]To whom correspondence may be addressed. Email: rothenburg@ucdavis.edu.

This article contains supporting information online at http://www.pnas.org/lookup/suppl/doi:10.1073/pnas.2115354119/-/DCSupplemental.

Published May 12, 2022.

PKR exerts its antiviral effect by phosphorylating the alpha subunit of the translation initiation factor (eIF2) at residue serine 51, thus inhibiting cap-dependent translation and inducing apoptosis (11, 12). eIF2α-mediated translational repression can have different effects on protein expression, including i) the reduction of protein expression by the inhibition of cap-mediated RNA translation (13); ii) the increased translation of RNAs that are eIF2α independent [e.g., RNAs containing some internal ribosome-entry sites or stem-loops that can directly recruit ribosomes and translation factors (14)]; iii) the increased expression of RNAs that contain inhibitory upstream open reading frames (ORFs) (15); and iv) the activation of signaling pathways through the enhanced turnover of inhibitor proteins with a short half-life (16, 17). PKR alsoregulates nuclear factor kappa B (NF-κB) through either interactions with the I kappa B kinase complex (IKK) (18, 19) or through the rapid turnover of its inhibitor IκB (16, 20).

NF-κB is a family of five structurally related, inducible transcription factors that regulate inflammatory, innate, and adaptive immune responses in mammals (21, 22). Under resting conditions, inactive NF-κB monomers are held in cytoplasmic protein complexes that include the short-lived inhibitor IκB. In the canonical activation pathway, IKK is activated by a variety of different inflammatory stimuli including cytokines and microbial components (23). Activated IKK then phosphorylates IκBα, targeting it for ubiquitin-mediated degradation, which results in the release of NF-κB proteins. These monomers rapidly translocate to the nucleus, dimerize, and then induce transcription of target genes. These target genes include the *NFKBIA* gene, which encodes IκBα, and proinflammatory genes, as well as tumor necrosis factor alpha (TNFα), interleukin (IL)-1, IL-6, and IL-8 (24, 25). Once resolution of the stimulus is achieved, the concurrent transcription of IκBα induces a negative feedback loop to rapidly inactivate NF-κB (26, 27).

In this study, we demonstrate that the MYXV PKR antagonist M156 regulates the NF-κB–IκBα complex and NF-κB–dependent inflammatory responses via differential inhibition of the PKR–eIF2α phosphorylation pathway. When PKR was either completely inhibited or fully activated, very little translation of NF-κB–induced target genes was observed. Surprisingly, European rabbit PKR was only partially inhibited by M156, despite the severe disease caused by MYXV in these animals. This partial inhibition promoted transcription of NF-κB target genes and translation of downstream effector molecules, presumably due to more rapid loss of the short-lived IκBα relative to effector molecules. Taken together, these findings provide compelling evidence that, at least in the case of MYXV, maladaptation of viral immune regulators to a new host can contribute to an increased proinflammatory response.

Results

M156 Inhibits PKR from Its Natural Host with Higher Efficiency Than European Rabbit PKR. In a previous study, M156 only inhibited PKR from the nonnative host European rabbit but did not inhibit PKR from seven other tested mammals (8). An important outstanding question was how inhibition of European rabbit PKR compared to inhibition of PKR from a natural MYXV host. To answer this, we first cloned PKR from the riparian brush rabbit (*S. bachmani riparius*). Total RNA was prepared from the muscle and connective tissues of rabbit paws from four individual brush rabbits that died in the field during the Riparian Brush Rabbit Project recovery program and were recovered in Stanislaus and San Joaquin counties (California). The full PKR ORF was successfully amplified and cloned by RT-PCR with primers adjacent to the ORF from three of these rabbits. Brush rabbit PKR showed 96% and 93% sequence identity compared to European rabbit PKR on the nucleotide and protein level, respectively. Amino acid differences between the two rabbit PKRs appeared to cluster in distinct regions (*SI Appendix*, Fig. S1*A*). This observation is supported by a sliding window analysis for the rate of accumulation of nonsynonymous to synonymous substitutions, which showed three distinct peaks with values >1 (*SI Appendix*, Fig. S1*B*). Next, we compared the sensitivities of each rabbit PKR to M156 inhibition using an established luciferase-based reporter (LBR) assay (28). In this assay, PKR-deficient HeLa cells were transiently cotransfected with a luciferase reporter, PKR, and potential PKR inhibitors. In this assay, PKR is activated by dsRNA that is formed by overlapping transcripts generated from the transfected plasmids (29), and luciferase expression serves as a proxy to quantify relative translation (28). Whereas M156 alone did not substantially alter luciferase expression, cotransfection of rabbit PKRs with M156R led to significantly increased luciferase expression, indicating PKR inhibition by M156. Notably, brush rabbit PKR was significantly better inhibited than European rabbit PKR by M156 (Fig. 1*A*). Both rabbit PKRs were expressed at comparable levels after transfection (*SI Appendix*, Fig. S1*C*).

To test if cells of rabbit origin also show higher inhibition of brush rabbit PKR by M156, we used the rabbit-derived cell line RK13 to generate a PKR knockout (ko) cell line using CRISPR–Cas-9 (*SI Appendix*, Fig. S2*A*). No PKR expression was detected in this cell line even after interferon treatment (*SI Appendix*, Fig. S2 *B* and *C*). In the RK13-PKR^{ko} cells, MYXV lacking PKR inhibitors M029 and M156 was able to replicate (*SI Appendix*, Fig. S2*D*). The LBR assay in these cells also showed that M156 inhibited brush rabbit PKR stronger than European rabbit PKR (*SI Appendix*, Fig. S3), confirming the results from the HeLa cells and confirming that cell lines of human and rabbit origin behave similarly in this LBR assay. For subsequent experiments, we focused on human-derived cells to take advantage of the wider array of available reagents.

To test whether brush rabbit PKR is more sensitive to pseudosubstrate inhibition in general, we cotransfected HeLa-PKR^{ko} cells either with rabbit PKR with an increasing amount of M156R or vaccinia virus K3L, the latter of which was previously shown to be an effective inhibitor of European rabbit PKR (30). Both M156 and K3 inhibited rabbit PKRs in dose-dependent manners. Whereas M156 inhibited brush rabbit PKR significantly better at all tested concentrations, no substantial differences were observed for K3, showing that both rabbit PKRs were comparably sensitive to K3 inhibition (Fig. 1 *B* and *C*).

We also compared PKR inhibition by M156 from the Californian MYXV California/San Francisco 1950 (MSW) strain because it is different from the M156 from the Lu strain, which we previously studied (75% sequence identity) (8). M156 from the MYXV Lu and the MSW strains showed comparable inhibition of brush rabbit and European rabbit PKRs, respectively. Taken together, these results demonstrated that M156 was a more efficient inhibitor of PKR from the natural host and that European rabbit PKR was inhibited suboptimally. Strikingly, it further shows that the level of PKR inhibition by M156 did not positively correlate with the described virulence of MYXV in its rabbit hosts.

Modulation of PKR-Induced NF-κB Activity by M156. We hypothesized that the dissimilar inhibition of PKR might result in differential activation of the proinflammatory transcription factor NF-κB. This pathway can be activated by PKR and other

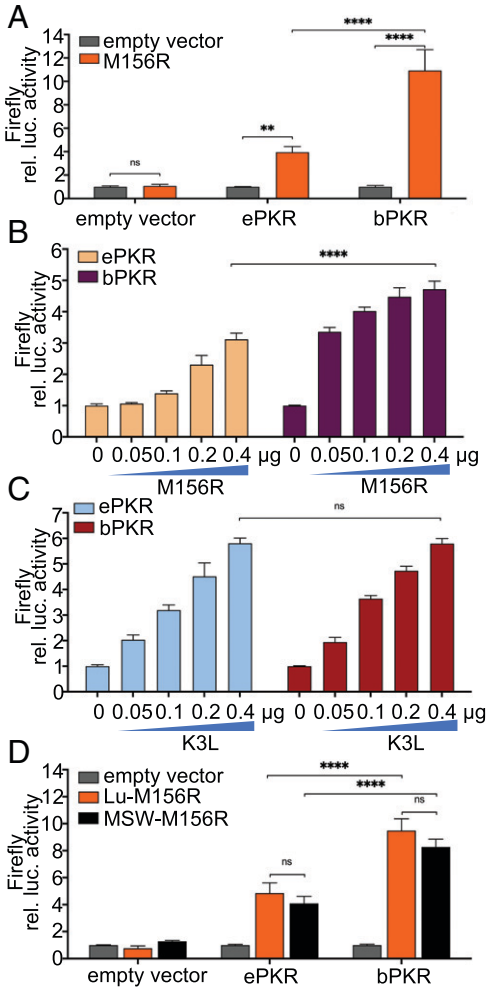

Fig. 1. Differential inhibition of European rabbit and brush rabbit PKR by M156. (*A*) HeLa-PKR^{ko} cells were transfected with expression vectors for firefly luciferase reporter (0.05 μg), M156 (0.4 μg), and PKR (0.2 μg) from either European rabbits (ePKR) or brush rabbits (bPKR). Luciferase activity was measured 48 h post transfection (hpt) and normalized to the empty vector control in each group. (*B* and *C*) ePKR or bPKR (0.2 μg) was cotransfected with increasing amounts of M156R (*B*) or VACV K3L, indicated in the figure (*C*), along with the firefly luciferase reporter (0.05 μg). Luciferase activity was determined 48 hpt. (*D*) Lu-M156R (0.4 μg) or MSW-M156R (0.4 μg) was cotransfected with vectors encoding firefly luciferase (0.05 μg), ePKR (0.2 μg), or bPKR (0.2 μg) for 48 h. Relative luciferase (rel. luc.) activity is shown. Experiments were performed in triplicate, and the results are representative of three independent experiments. Error bars indicate SDs. Asterisks denote *P* values: $^{**}P < 0.01$; $^{****}P < 0.0001$. ns, not significant.

eIF2α kinases through the depletion of the NF-κB inhibitor IκBα, which has a short half-life and is therefore disproportionately depleted after translational inhibition (17). To test this hypothesis, we first transiently transfected HeLa-PKR ^{ko} cells with increasing amounts of either European rabbit PKR or brush rabbit PKR and measured the translational inhibition of PKRs by the LBR assay. We focused on the cells of human origin because more reagents are available to study the NF-κB pathway. Simultaneously, we measured the expression of IκBα and the NF-κB subunit p65 by Western blot analysis. Increasing amounts of either European rabbit PKR or brush rabbit PKR led to comparable translational inhibition as observed by the LBR assay (*SI Appendix*, Fig. S4). Increasing amounts of either PKR also resulted in comparably decreased levels of IκBα, whereas p65 or β-actin (control) levels were barely affected (Fig. 2 *A* and *B*). Lower IκBα protein was not due to a reduction of IκBα transcripts, as those actually increased after PKR transfection (Fig. 2 *C* and *D*). This observation is consistent with reports that the IκBα encoding gene itself is activated by NF-κB (31, 32). We next assessed whether M156 can modulate the PKR-induced transcription of the NF-κB–activated proinflammatory genes, like TNFα and IL-6. Transfection of European rabbit PKR or brush rabbit PKR alone led to increased levels of TNFα and IL-6 transcripts (Fig. 2 *E* and *F*). Whereas cotransfection of M156R with European rabbit PKR led to only moderately reduced TNFα and IL-6 messenger RNA (mRNA) levels, cotransfection of M156R with brush rabbit PKR resulted in strongly reduced TNFα and IL-6 mRNA levels (Fig. 2 *E* and *F*). We also used an NF-κB–dependent reporter assay to monitor NF-κB–dependent responses after differential PKR inhibition. After 48 h, cotransfection of

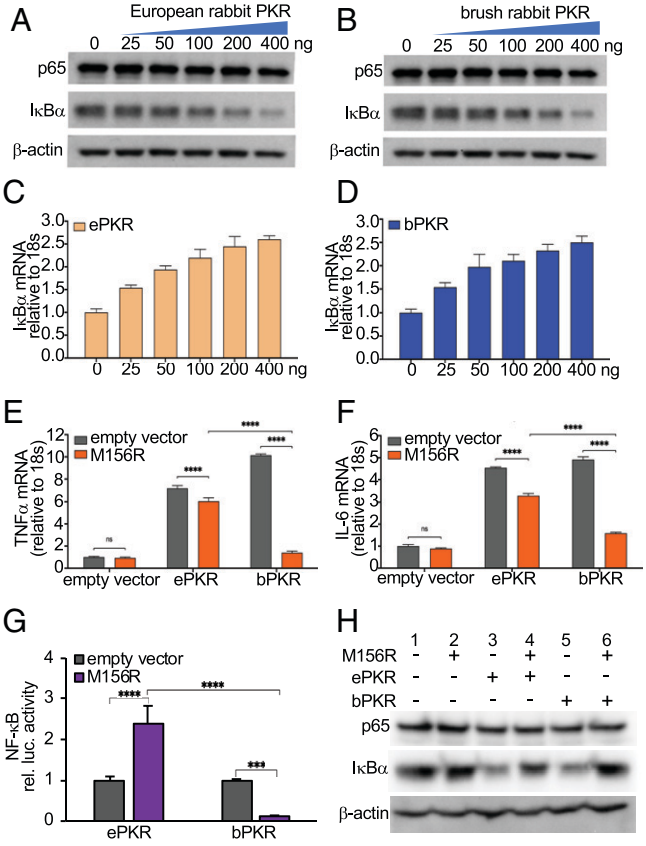

Fig. 2. Modulation of NF-κB activity by differential inhibition of rabbit PKRs. (*A–D*) HeLa-PKR^{ko} cells were transfected with increasing amounts of European rabbit PKR (ePKR; *A* and *C*) or brush rabbit PKR (bPKR; *B* and *D*) as indicated. After 24 h, total protein lysates were collected and subjected to Western blot analyses for NF-κB–p65, IκBα, and β-actin (*A* and *B*). IκBα mRNA levels (*C* and *D*) were measured by qRT-PCR at 24 h post transfection (hpt) in parallel experiments. (*E* and *F*) HeLa-PKR^{ko} cells were cotransfected with M156R (0.3 μg) and either ePKR (0.3 μg) or bPKR (0.3 μg). After 24 h, total RNA was isolated from the transfected cells and subjected to qRT-PCR for TNFα (*E*) and IL-6 (*F*). (*G*) HeLa-PKR^{ko} cells were cotransfected with expression vectors encoding M156 (0.3 μg), the indicated PKRs (0.3 μg), and both the NF-κB–responsive firefly luciferase and constitutively active renilla luciferase reporters (0.05 μg each). After 48 h, firefly and renilla luciferase activities were measured. The results are representative of three independent experiments. (*H*) In order to analyze the effects of M156 on PKR-dependent IκB levels, we cotransfected HeLa-PKR^{ko} cells with M156R and ePKR or bPKR and stimulated cells with poly(I:C) to mimic dsRNA production during a virus infection. In details, HeLa-PKR^{ko} cells were cotransfected with M156R (0.8 μg) and the indicated PKRs (0.4 μg). After 16 h, cells were stimulated with 5 μg/mL poly(I:C) for 8 h. At 24 hpt, total proteins were isolated and subjected to immunoblotting using antibodies specific for NF-κB–p65, IκBα, and β-actin. Error bars indicate SDs. Asterisks denote *P* values: $^{***}P < 0.001$; $^{****}P < 0.0001$. ns, not significant; rel. luc., relative luciferase.

M156R with European rabbit PKR resulted in a significant increase in luciferase expression as compared to European rabbit PKR-only transfected cells. In contrast, cotransfection of M156R with brush rabbit PKR resulted in significantly decreased luciferase expression compared to brush rabbit PKR-only transfected cells (Fig. 2*G*). Similar, although not as pronounced, differences were observed 24 h after transfection (*SI Appendix*, Fig. S5*A*). In order to analyze the effects of M156 on PKR-dependent IκB levels, we cotransfected HeLa-PKR^{ko} cells with M156R and European rabbit PKR or brush rabbit PKR and stimulated cells with polyinosinic:polycytidylic acid [poly(I:C)] to simulate dsRNA production during virus infection. Transfection of either European rabbit PKR or brush rabbit PKR alone led to strongly reduced IκBα levels when compared to the empty vector and M156R-only controls (Fig. 2*H*, lanes 3 and 5). Whereas cotransfection of brush rabbit PKR with M156R resulted in high IκBα levels (lane 6), comparable to the controls, transfection of European rabbit PKR reduced IκBα levels (lane 4) below the control samples (lanes 1 and 2), but not as much as PKR alone (lane 3). Taken together, these results show that intermediate PKR inhibition can result in increased NF-κB pathway activation.

PKR-Dependent IκBα Depletion and NF-κB Activation during MYXV Infection. To test the role of PKR in IκBα degradation during MYXV infection, we infected both PKR-competent and PKR^{ko} HeLa and A549 cells with a MYXV construct lacking its two PKR inhibitors, M029 and M156 (MYXVΔM029LΔM156R). This virus expresses enhanced green fluorescent protein (EGFP) for easier monitoring of virus infection. At multiple times after infection, we assayed these cells for phosphorylated PKR, total PKR, phosphorylated eIF2α, total eIF2α, p65, IκBα, and the viral proteins M-T7 and M130 by Western blot analyses. The absence of PKR in the HeLa- and A549-PKR^{ko} cells was confirmed using anti-PKR antibodies (Fig. 3) Virus infection caused phosphorylation of both PKR and eIF2α in the wild-type (WT) cells, which was most prominent between 8 and 24 h post infection (hpi), but not in the PKR-deficient cells. Virus infection also led to a PKR-dependent loss of IκBα expression, which was most prominent 12 hpi. IκBα expression recovered 48 hpi, and this recovery correlated with lower levels of PKR and eIF2α phosphorylation. In the PKR-deficient cells, a weaker and later (24 to 48 h) decrease in IκBα expression was observed. These data suggest that there were two phases of NF-κB activation, a fast PKR-dependent loss of IκBα expression followed by a slower and less prominent PKR-independent loss of IκBα expression during infection. To determine whether MYXV caused a productive infection in these cell lines, we probed for the expression of MYXV M-T7 and M130, which are early and late proteins, respectively. In HeLa WT cells, some M-T7 was detected but not M130, indicating an abortive infection. In contrast, both proteins were detected in HeLa-PKR^{ko} cells, indicating productive infection. In both A549 cell lines, little M-T7 and no M130 were detected, indicating nonproductive infections. In agreement, strong EGFP signals were only detected in HeLa-PKR^{ko} cells (*SI Appendix*, Fig. S6). To determine whether PKR also directly influences the canonical NF-κB pathway, we tested activity of the NF-κB–dependent luciferase reporter in response to increasing amounts of TNFα in WT and PKR-deficient HeLa cells and found no substantial differences in NF-κB activation, indicating that PKR did not affect TNFα-induced activation of NF-κB (*SI Appendix*, Fig. S7).

We next tested whether IκBα depletion during infection could be inhibited by treatment with cytosine β-d-arabinofuranoside (AraC), which inhibits poxviral DNA replication and therefore also inhibits intermediate and late gene transcription. As a result, AraC treatment leads to a strong reduction in the formation of viral dsRNA, the activator of PKR during infection (33, 34). In HeLa and A549 cells, AraC treatment reduced PKR and eIF2α phosphorylation during infection with MYXVΔM029LΔM156R and partially restored IκBα expression (Fig. 4 *A* and *B*). We also determined mRNA expression levels of the proinflammatory NF-κB target genes TNFα and IL-6 by qRT-PCR during infection in WT and PKR-deficient HeLa and A549 cells. Infection of the PKR-deficient cell lines with MYXVΔM029LΔM156R led to an increase in TNFα and IL-6 transcript levels. In the PKR-competent cell lines, this increase was significantly higher, whereas AraC treatment led to transcript levels that were comparable to that observed in the PKR-deficient cell lines (Fig. 4 *C*–*F*). These data support the notion of PKR-dependent and independent mechanisms of NF-κB activation during infection.

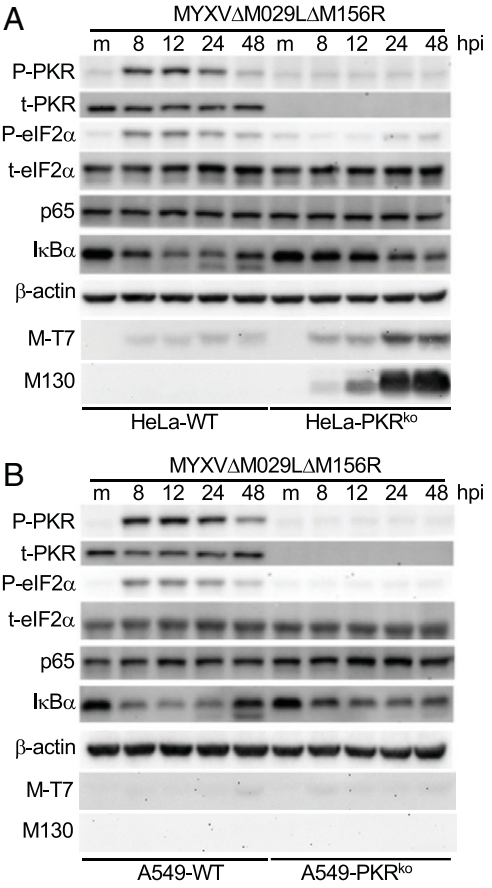

Fig. 3. Activated PKR-mediated IκBα depletion during MYXV infection. (*A* and *B*) HeLa-WT or PKR^{ko} (*A*) and A549-WT or PKR^{ko} (*B*) cells were infected with MYXVΔM029LΔM156R at an MOI of 3 for 8, 12, 24, or 48 h. Total protein lysates were collected and subjected to Western blot analyses for phosphorylated PKR (P-PKR), total PKR (t-PKR), phosphorylated eIF2α (P-eIF2α), total eIF2α (t-eIF2α), NF-κB–p65, IκBα, and β-actin as well for MYXV M-T7 (early protein) and M130 (late protein). Lysates of mock-infected control cells (m, collected at 8 h) were included as controls.

Modulation of Proinflammatory Gene Expression by M156 during Infection of Rabbit PKR-Expressing Cells. Next, we tested whether the expression of proinflammatory genes can be affected by M156 during virus infection. We stably transfected PKR-deficient HeLa cells with either empty vector or European rabbit PKR or brush rabbit PKR under the control of the

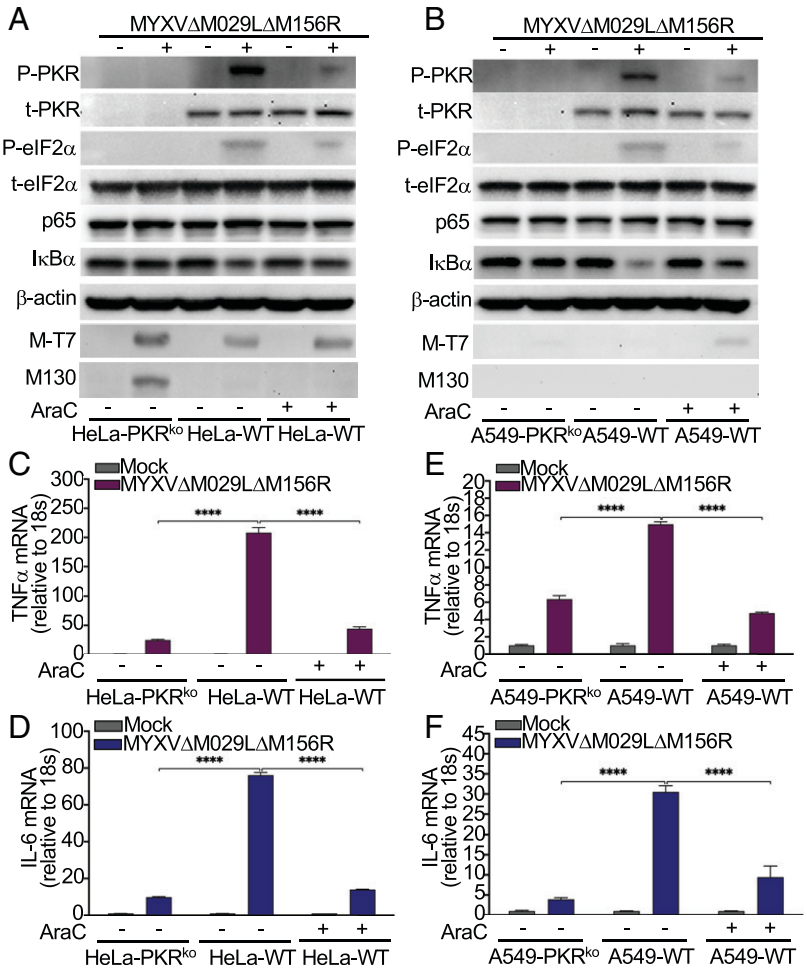

Fig. 4. PKR-mediated amplification of proinflammatory cytokine expression during MYXV infection. (*A–F*) HeLa-WT and HeLa-PKR^{ko} (*A*, *C*, and *D*) or A549-WT and A549-PKR^{ko} (*B*, *E*, and *F*) were infected with MYXVΔM029LΔM156R at an MOI of 3. As indicated, HeLa-WT or A549-WT cells were also treated with 50 μg/mL AraC. Total protein lysates were collected at 8 hpi to monitor the expression of indicated proteins using indicated antibodies as in Fig. 3 *A* and *B*. At 12 hpi, the total RNA was isolated from the indicated cells and subjected to qRT-PCR for TNFα (*C* and *E*) and IL-6 (*D* and *F*), respectively. P-eIF2α, phosphorylated eIF2α; P-PKR, phosphorylated PKR; t-eIF2α, total eIF2α; t-PKR, total PKR. Error bars indicate SDs. Asterisks denote *P* values: ****$P < 0.0001$.

human PKR promoter and isolated monoclonal cells that expressed European rabbit PKR and brush rabbit PKR at a comparable level (Fig. 5*A*). These cells were then infected with MYXVΔM029L, MYXVΔM029LΔM156R, and the revertant virus MYXVΔM029LΔM156R/M156R^{rev}. In HeLa-PKR^{ko} control cells, comparable TNFα and IL-6 induction was observed for all virus infections (Fig. 5 *B* and *C*). In European rabbit PKR– and brush rabbit PKR–expressing cells, infection with MYXVΔM029LΔM156R led to a strong induction of both TNFα and IL-6. When brush rabbit PKR–expressing cells were infected with the M156-expressing viruses, we observed a strong reduction (~sixfold) in both TNFα and IL-6 levels, to levels comparable to the control cells. In contrast, European rabbit PKR–expressing cells infected with these viruses displayed only a twofold reduction in TNFα and IL-6 levels (Fig. 5 *B* and *C*). These results indicate that M156 only partially repressed European rabbit PKR–induced NF-κB activation, whereas it strongly inhibited brush rabbit PKR–induced NF-κB activation during infection. We also monitored EGFP production during MYXV infection by fluorescence microscopy (*SI Appendix*, Fig. S8). Whereas infection with all viruses led to high EGFP signals in HeLa-PKR^{ko} cells, little EGFP expression was observed in cells infected with MYXVΔM029LΔM156R, indicating that virus replication was suppressed in cells expressing European rabbit or brush rabbit PKR. In the presence of M156, we observed strong EGFP signals in brush rabbit PKR–expressing cells, comparable to that observed in the parental HeLa-PKR^{ko} cells, while we observed intermediate EGFP signals in European rabbit PKR–expressing cells. This difference in EGFP expression indicated that brush rabbit PKR was strongly inhibited, while European rabbit PKR was incompletely suppressed by M156.

Hyperactive M156 Fails to Induce European rabbit PKR–Mediated NF-κB Activation. These preceding data support our hypothesis that preferential depletion of IκBα due to intermediate inhibition of European rabbit PKR by M156, but not strong inhibition of brush rabbit PKR, results in NF-κB activation. This hypothesis predicts that a hyperactive M156 also would not induce European rabbit PKR–mediated NF-κB activation by fully preventing translational shutoff rather than allowing some translation to occur. To test this hypothesis, we employed a random mutagenesis yeast screen of M156 to identify hyperactive mutants. We used a previously described yeast strain that contains chromosomally integrated, galactose-inducible European rabbit PKR and transformed it with two libraries of mutagenized M156 that were each created from ~42,000 *Escherichia coli* transformants. The finding that VACV K3 inhibited PKR-mediated toxicity better than M156 indicated the feasibility of this approach (8). In total, we selected 2,900 yeast colonies that

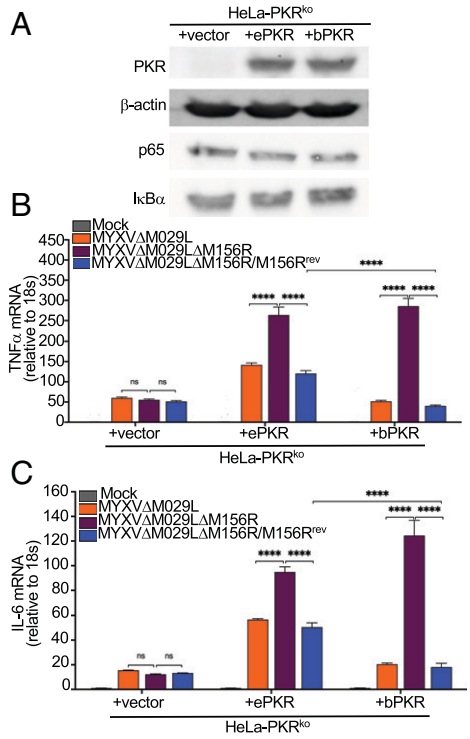

Fig. 5. PKR-dependent modulation of proinflammatory gene expression during infection of MYXV infection. (*A*) HeLa-PKR^{ko} cells were stably transfected with empty vector, European rabbit PKR (ePKR), or brush rabbit PKR (bPKR) under the control of the human PKR promoter. The expression of ePKR and bPKR was measured by Western blot analyses using anti-PKR antibody. (*B* and *C*) Congenic HeLa-PKR^{ko} cell lines, which stably express vector control, ePKR, or bPKR were mock infected or infected with MYXVΔM029L, MYXVΔM029LΔM156R, and MYXVΔM029LΔM156R/M156R$^{revertant(rev)}$ at an MOI of 3. At 12 hpi, total RNA was isolated from the indicated cell lines and subjected to qRT-PCR for TNFα (*B*) and IL-6 (*C*). Error bars indicate SDs. Asterisks denote *P* values: ****$P < 0.0001$. ns, not significant.

were transformed with either library and performed replica plating. Plasmids of transformants that showed substantially better growth than those transformed with WT M156 were isolated, sequenced, and retransformed into the European rabbit PKR–expressing yeast strain. Transformants with single mutations in M156R at four different sites were identified, which facilitated better yeast growth: K21Q (identified twice from library 1), E28V (identified once from library 1 and twice from library 2), N39D (identified once from library 1), and Q42L (identified three times from library 1) (Fig. 6*A*). Positions of these mutated amino acids projected on the structure of M156 showed that two of the residues (N39 and Q42) were adjacent to residue Y40, which corresponds to the phosphorylation site in eIF2α and which has also been shown to be phosphorylated by human PKR in M156 (35) (Fig. 6 *B* and *C*). K21 corresponds to Y32 of eIF2α, which was found to be in direct contact with PKR in a cocrystal structure (36). When these mutations were introduced into M156R for the LBR assay, M156-K21Q, N39, and Q42 showed significantly increased inhibition of European rabbit PKR compared to WT M156 (Fig. 6*D*). Because residue K21 was identified as critical for PKR inhibition, we substituted it with every amino acid and measured the effect in the LBR assay. We observed a spectrum of PKR inhibition, ranging from no inhibition, to inhibition comparable to WT M156, to enhanced inhibition comparable to M156-K21Q (K21M and K21Y) (Fig. 6*E*).

We next compared the effects of the hyperactive M156-K21Q and the naturally occurring hypoactive M156-L71P variant on European rabbit PKR and brush rabbit PKR in the LBR assay and in dual luciferase assays using a reporter containing either the ATF-4 upstream open-reading frame (uORF) or the NF-κB–responsive promoter. These M156 mutants were expressed comparably to WT M156 (*SI Appendix*, Fig. S9). M156-K21Q increased luciferase activity only when cotransfected with European rabbit PKR but not with brush rabbit PKR (Fig. 6*F*). In the ATF4-uORF assay, firefly luciferase activity is stimulated by eIF2α phosphorylation (15). In this assay, M156-K21Q led to significantly less luciferase activity than WT M156 only for European rabbit PKR but had no major effects on brush rabbit PKR (Fig. 6*G*). Thus, as predicted, the results inversely correlated with the LBR assay. In the NF-κB activity reporter assay, cotransfection of only European rabbit PKR with WT M156 but not M156-K21Q led to elevated luciferase activity, whereas no significant difference was detected for brush rabbit PKR at 48 h (Fig. 6*H*) and 24 h (*SI Appendix*, Fig. S5*B*). Western blot analyses revealed that cotransfection of European rabbit PKR with M156-K21Q followed by poly(I:C) stimulation resulted in higher IκBα expression levels (Fig. 6*I*, lane 4) than when it was cotransfected with WT M156 (lane 3), which resulted in intermediate IκBα expression levels.

Discussion

MYXV infection of European rabbits is one of the best-defined examples of host–virus coevolution on the population level (4). This coevolution is at least in part due to the fact that MYXV gains substantial virulence as a consequence of host switching, resulting in very strong selective pressure on both the host and the virus. Previous work defining the molecular interactions between MYXV and host proteins was primarily performed using cell lines and proteins derived from humans or European rabbits; however, these molecular host–virus interactions had not been well studied in the context of its natural hosts. In this study, we show that, paradoxically, MYXV M156 inhibited brush rabbit PKR much more efficiently than European rabbit PKR, even though MYXV causes a relatively benign, localized lesion in brush rabbits but is highly virulent in European rabbits (2, 3). This observation is even more surprising in light of our previous work demonstrating that attenuation of MYXV isolates from Australia correlated with the emergence of a loss-of-function mutation in M156R against European rabbit PKR (8).

Here, we demonstrate that the moderate inhibition of European rabbit PKR by M156 allowed translation of a NF-κB–activated reporter, whereas complete inhibition of brush rabbit PKR by M156 did not. Furthermore, either hyperactive or hypoactive M156 failed to induce European rabbit PKR–mediated NF-κB reporter expression. In the infection experiments, eIF2α phosphorylation coincided with a rapid loss of the NF-κB inhibitor IκBα and thus activation of NF-κB–mediated transcription. The maladaptation between M156 and PKR derived from the aberrant European rabbit host resulted in the partial PKR activation and intermediate phosphorylation of eIF2α. As a consequence, some translation could still proceed, permitting expression of NF-κB–transcribed cytokines (Fig. 7). In contrast, fully activated PKR led to high eIF2α phosphorylation levels, which not only resulted in strong NF-κB activation but also inhibited translation of the induced mRNAs. A similar outcome was seen with complete PKR inhibition, where NF-κB was not activated and thus IκBα was not depleted. Taken together, these results demonstrate that intermediate inhibition of PKR is able to functionally activate the NF-κB pathway and still allow translation of NF-κB target

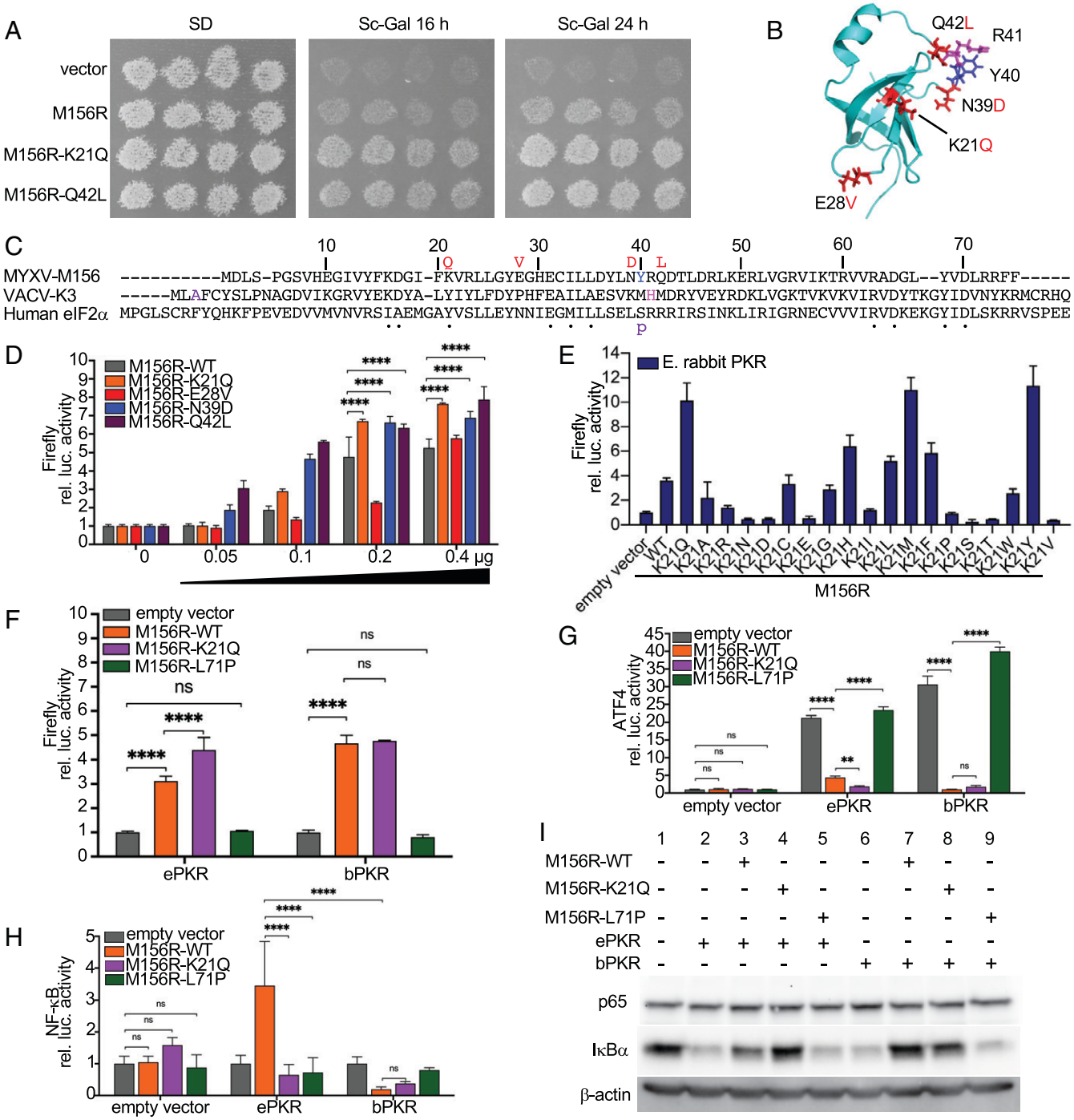

Fig. 6. Activation of the NF-κB pathway after intermediate inhibition of PKR by M156. (*A*) Plasmids encoding empty vector, M156, M156-K21Q, or M156-Q42L under the control of a galactose-inducible promoter were transformed into a yeast strain that has European rabbit PKR stably integrated at the LEU2 locus under the control of the GAL-CYC1 hybrid promoter. For each transformant, four colonies were purified and grown under noninducing (SD) or inducing conditions (Sc-Gal) at 30 °C for 16 or 24 h. (*B*) Solution structure of M156 (35). Positions of mutations identified in a random mutagenesis screen in M156 that conferred hyperinhibition of European rabbit PKR (ePKR) in yeast growth assays are shown in red. Residues Y40 and R41 are also highlighted. (*C*) Multiple sequence alignment of MYXV-Lu M156, VACV K3, and human eIF2α. Mutations that conferred hyperactivity of M156 in the yeast assay are shown in red. Y40 is shown in blue. H47 in VACV-K3, which corresponds to R41 in M156, is shown in magenta. The P denotes the phosphorylated sites in eIF2α and M156. Dots denote eIF2α residues that contact human PKR in the cocrystal structure (36). (*D*) HeLa-PKR^{ko} cells were cotransfected with increasing amounts of either M156R-WT or the indicated M156R mutants, firefly luciferase (0.05 μg), and ePKR (0.2 μg). At 48 h post transfection (hpt), luciferase activity was measured. (*E*) HeLa-PKR^{ko} cells were cotransfected with expression vectors encoding firefly luciferase (0.05 μg), with the indicated M156R mutants (0.4 μg) and ePKR (0.2 μg). Luciferase activity was measured 48 hpt. (*F*) ePKR (0.2 μg) or brush rabbit PKR (bPKR) (0.2 μg) and firefly luciferase reporter (0.05 μg) were cotransfected with either M156R or the indicated mutants of M156R (0.4 μg). (*G* and *H*) HeLa-PKR^{kd} cells were cotransfected with expression vectors encoding MYXV M156 (0.4 μg) or indicated M156 mutants (0.4 μg), ePKR or bPKR (0.2 μg), renilla luciferase (0.05 μg), along with ATF4-firefly luciferase (0.05 μg), which contains the mouse ATF4 mRNA-5′ untranslated region sequence (*G*) or NF-κB–dependent firefly luciferase (0.05 μg) (*H*). After 48 h, firefly luciferase activities were measured. Results shown are representative of three independent experiments. Error bars indicate the SDs from three independent transfections. (*I*) M156R (0.8 μg) or indicated M156R mutants were cotransfected with indicated PKRs (0.4 μg) in the HeLa-PKR^{ko} cells. After 16 h, cells were stimulated with 5 μg/mL poly(I:C) for 8 h. At 24 hpt, total protein lysates were analyzed by immunoblotting with the indicated antibodies. Error bars indicate SDs. Asterisks denote *P* values: $^{**}P < 0.01$; $^{****}P < 0.0001$. ns, not significant; rel. luc., relative luciferase.

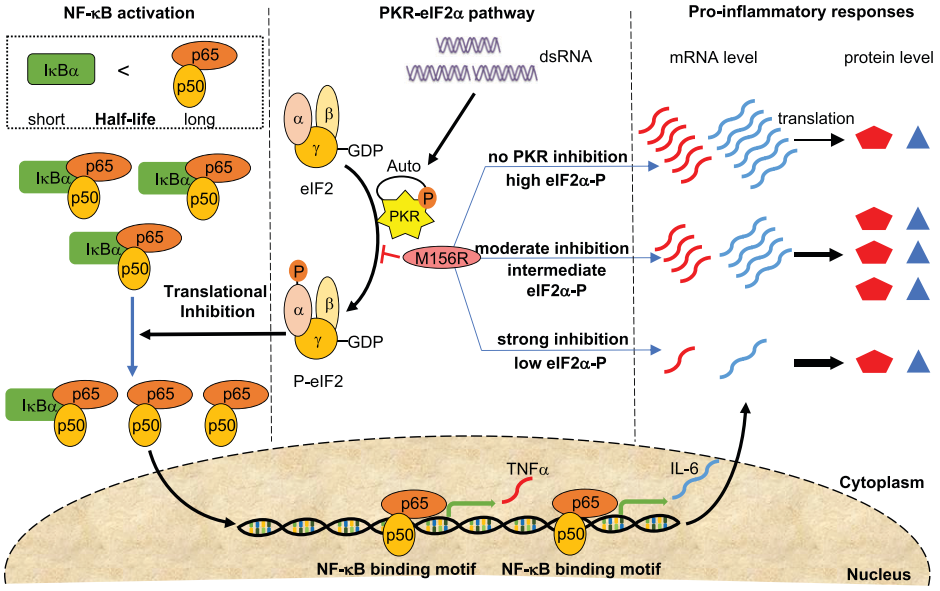

Fig. 7. Effects of intermediate PKR inhibition on the NF-κB pathway. Red and blue squiggles represent mRNA. Red pentagons and blue triangles represent proteins. P mark phosphorylated proteins. P-eIF2, phosphorylated eIF2; GDP, guanosine diphosphate.

genes. This limited, cap-dependent translation after activation of the PKR pathway might profoundly shape other cellular responses.

There are two different mechanisms that have been described for NF-κB activation by PKR: i) direct association of PKR with IκBα or components of the IKK complex (18, 37–41) and ii) indirectly due to translational repression resulting in more rapid depletion of short–half-life proteins relative to more stable proteins. This second mechanism has been demonstrated for the eIF2α kinases PKR, GCN2, and PERK in response to viral infections or other cell stressors. When these kinases are activated, the subsequent translational repression depletes the short–half-life protein IκBα more rapidly than NF-κB, thus relieving its inhibitory effect on NF-κB and activating the NF-κB pathway (16, 17, 20, 42, 43). Our observation that NF-κB activation was blocked by strong PKR inhibition of both rabbit PKRs indicates that the enzymatic activity of PKR and possibly the phosphorylation status of eIF2α are important for this process. Both brush rabbit and European rabbit PKR caused comparable activation of NF-κB in the absence of PKR inhibitors. In transfection assays, both PKRs led to reduced IκBα protein levels and increased mRNA expression of the NF-κB targets IκBα, TNFα, and IL-6. Similarly, transgenic HeLa cells that express either brush rabbit or European rabbit PKR instead of endogenous PKR had a comparable, PKR-dependent induction of TNFα and IL-6 when infected with MYXV devoid of its two native PKR inhibitors. Using two different PKR-deficient cell lines, we also demonstrated that MYXV infection can induce the NF-κB pathway in both a PKR-dependent and a PKR-independent manner. The PKR-dependent IκBα depletion occurred relatively rapidly and reached a maximum at ∼12 hpi, whereas the PKR-independent IκBα depletion was not as pronounced and occurred more slowly through an unknown mechanism (Fig. 3). Induction of TNFα and IL-6 was also more pronounced when the NF-κB pathway was activated through the PKR-dependent mechanism relative to PKR-independent NF-κB activation. These data emphasize the important role of PKR in NF-κB activation during poxvirus infection.

One of the most profound differences between brush rabbits and European rabbits during the course of MYXV infection is that MYXV produces a localized skin infection in its natural host, while in European rabbits it disseminates systemically. While many virus spillover events are likely dead ends due to maladaptation between host and pathogen (44), here we demonstrated an example of molecular maladaptation that correlates with increased host virulence and virus dissemination in the aberrant host. Because European rabbit PKR was only partially inhibited by M156, the functional activation of NF-κB and the resulting expression of inflammatory cytokines such as IL-6 and TNFα may promote the systemic spread of MYXV in European rabbits. For example, in MYXV infection of European rabbits, leukocytes play an essential role in the systemic dissemination of viruses (4, 45). In fact, the NF-κB–induced cytokine TNFα "activates" the endothelium to initiate the multistep adhesion cascade to recruit neutrophils (46, 47). Therefore, the continued expression of TNFα in MYXV-infected European rabbits indicates a potential mechanism to initiate and promote systemic spread of the virus in European rabbits and provides a possible explanation for the different disease outcomes in European and brush rabbits, which will be addressed in subsequent studies.

An important role for NF-κB in poxvirus infection is also supported by the presence of many NF-κB pathway inhibitors in poxviruses (48, 49) and a recent study that implicated NF-κB activation by ORF120 as a critical virulence factor for Orf virus (50). The maladaptation of M156 and PKR as a potential contributor to virulence is supported by our previous observation of an M156 loss-of-function mutation evolving in a substantial proportion of Australian rabbits, which correlated with MYXV attenuation (8). As an extension of this observation, our work also supports the hypothesis that evolution of a hyperactive M156 should have a similar attenuating effect on MYXV disease in European rabbits and may evolve in natural populations as well. Together with earlier studies, these data show that PKR-dependent pathways in infection should be considered when studying NF-κB activation.

Overall, our results show that that PKR activation is not an "on-off switch" for translation. Rather, PKR may initiate a spectrum of translation inhibition, at least in certain situations. This attenuated translation may result in differential proteomic profiles during infection based on half-life or other intrinsic properties of the proteins, such as the changes to TNFα and

IL-6 that we demonstrated in this study. Currently, it is unclear whether this phenomenon is specific to the rabbit/MYXV system or if it is a more generalizable phenotype. If this is a general mechanism of a more measured translational shutoff by PKR, this may represent a mechanism to fine-tune the intracellular environment, which could conceivably be manipulated by either the host or the virus depending on context. Molecular maladaptations after host switches might lead to unanticipated consequences, as described here, and play crucial roles in influencing infection, virulence, and transmission and thus virus host range.

Materials and Methods

Plasmids, Yeast Strains, and Cell Lines. Cloning of European rabbit PKR and MYXV M156R was described previously (8). Brush rabbit PKR (GenBank accession No. OM831131), MSW-M156R, and M156R mutants were cloned into pSG5 for expression in mammalian cells. HeLa-PKR^{ko} cells [a kind gift of Adam Geballe, Fred Hutchinson Cancer Research Center, Seattle, WA (51)] were stably transfected with European rabbit PKR and brush rabbit PKR under the control of the human PKR promoter. See *SI Appendix, Materials and Methods* for details.

LBR Assays. Single or dual luciferase assays were performed as previously described (8). Briefly, 5×10^4 HeLa-PKR^{ko} cells or HeLa-PKR$^{knockdown(kd)}$ cells were seeded in 24-well plates 24 h prior to the experiment. Cells were transfected with the indicated plasmids using GenJet (Signagen) following the manufacturer's protocol. After 48 h, cell lysates were harvested using mammalian lysis buffer (GE Healthcare), and pGL3-firefly luciferase, NF-κB– or ATF4-firefly luciferase, and renilla luciferase were measured. See *SI Appendix, Materials and Methods* for details.

Western Blot Analyses. HeLa-PKR^{ko} cells were transfected with either European rabbit PKR or brush rabbit PKR alone or in combination with K3L, M156R, or M156R mutants. In separate experiments, 4×10^5 HeLa-WT, HeLa-PKR^{ko}, A549-WT, or A549-PKR^{ko} cells were seeded in 6-well plates and infected with MYXVΔM029LΔM156R at a multiplicity of infection (MOI) of 3 for the times indicated in the figures. Cells were lysed with 1% sodium dodecyl sulfate (SDS) in phosphate-buffered saline (VWR) and sonicated at 50% amplitude for 10 s twice. The lysates were separated by 12% SDS/polyacrylamide gel electrophoresis, blotted on polyvinylidene difluoride membranes, and incubated with diluted primary and secondary antibodies as described in *SI Appendix, Materials and Methods*.

qRT-PCR. Transfected or infected cells were collected and lysed with TRIzol Reagent (Invitrogen). Total cellular RNA was isolated using Direct-zol RNA Kits (Zymo Research); then complementary DNA was synthesized using protoScript II reverse transcriptase (NEB). qRT-PCR was performed using EvaGreen dye (Biotium) and measured using CFX Connect Real-Time PCR Detection System (Bio-Rad). See *SI Appendix, Materials and Methods* for details.

Yeast Growth Assays. Experiments were performed as previously described (8, 52). See *SI Appendix, Materials and Methods* for details.

Statistical Analysis. Statistical analyses were performed using Prism 8 Software (GraphPad). The data were analyzed using paired Student's *t* test. A P value of <0.05 was considered significant. $^*P < 0.05$, $^{**}P < 0.01$, $^{***}P < 0.001$, $^{****}P < 0.0001$; ns, not significant. All values are presented as the means ± SD.

Data Availability. The sequence for the brush rabbit PKR gene has been deposited to GenBank (accession no. OM831131). All study data are included in the article and/or *SI Appendix*.

ACKNOWLEDGMENTS. We thank Dr. Thomas Dever for helpful discussions and Drs. Patrick Kelly, Matthew Lloyd, Ron Wek, Charles Samuel, Adam Geballe, Bernard Moss, Thomas Dever, Bastian Opitz, and Grant McFadden for kindly provided materials and reagents. Parts of this work were included in the PhD dissertation of C.P. (53). This work was supported by Grant R01 AI114851 (to S.R.) from the National Institute of Allergy and Infectious Diseases.

Author affiliations: [a]Department of Medical Microbiology and Immunology, School of Medicine, University of California, Davis, CA 95618; and [b]Key Laboratory of Animal Epidemiology and Zoonosis, College of Veterinary Medicine, China Agricultural University, Beijing 100193, China

1. J. L. Geoghegan, E. C. Holmes, The phylogenomics of evolving virus virulence. *Nat. Rev. Genet.* **19**, 756–769 (2018).
2. D. C. Regnery, J. H. Miller, A myxoma virus epizootic in a brush rabbit population. *J. Wildl. Dis.* **8**, 327–331 (1972).
3. P. J. Kerr, S. M. Best, Myxoma virus in rabbits. *Rev. Sci. Tech.* **17**, 256–268 (1998).
4. P. J. Kerr, Myxomatosis in Australia and Europe: A model for emerging infectious diseases. *Antiviral Res.* **93**, 387–415 (2012).
5. K. Myers, Studies in the epidemiology of infectious myxomatosis of rabbits. II. Field experiments, August-November 1950, and the first epizootic of myxomatosis in the Riverine Plain of south-eastern Australia. *J. Hyg. (Lond.)* **52**, 47–59 (1954).
6. I. D. Marshall, F. Fenner, Studies in the epidemiology of infectious myxomatosis of rabbits. V. Changes in the innate resistance of Australian wild rabbits exposed to myxomatosis. *J. Hyg. (Lond.)* **56**, 288–302 (1958).
7. I. D. Marshall, G. W. Douglas, Studies in the epidemiology of infectious myxomatosis of rabbits. VIII. Further observations on changes in the innate resistance of Australian wild rabbits exposed to myxomatosis. *J. Hyg. (Lond.)* **59**, 117–122 (1961).
8. C. Peng, S. L. Haller, M. M. Rahman, G. McFadden, S. Rothenburg, Myxoma virus M156 is a specific inhibitor of rabbit PKR but contains a loss-of-function mutation in Australian virus isolates. *Proc. Natl. Acad. Sci. U.S.A.* **113**, 3855–3860 (2016).
9. E. Meurs *et al.*, Molecular cloning and characterization of the human double-stranded RNA-activated protein kinase induced by interferon. *Cell* **62**, 379–390 (1990).
10. F. Weber, V. Wagner, S. B. Rasmussen, R. Hartmann, S. R. Paludan, Double-stranded RNA is produced by positive-strand RNA viruses and DNA viruses but not in detectable amounts by negative-strand RNA viruses. *J. Virol.* **80**, 5059–5064 (2006).
11. S. Li *et al.*, Molecular basis for PKR activation by PACT or dsRNA. *Proc. Natl. Acad. Sci. U.S.A.* **103**, 10005–10010 (2006).
12. M. Dey *et al.*, Mechanistic link between PKR dimerization, autophosphorylation, and eIF2alpha substrate recognition. *Cell* **122**, 901–913 (2005).
13. T. E. Dever, Translation initiation: Adept at adapting. *Trends Biochem. Sci.* **24**, 398–403 (1999).
14. K. D. Fitzgerald, B. L. Semler, Bridging IRES elements in mRNAs to the eukaryotic translation apparatus. *Biochim. Biophys. Acta* **1789**, 518–528 (2009).
15. K. M. Vattem, R. C. Wek, Reinitiation involving upstream ORFs regulates ATF4 mRNA translation in mammalian cells. *Proc. Natl. Acad. Sci. U.S.A.* **101**, 11269–11274 (2004).
16. J. Deng *et al.*, Translational repression mediates activation of nuclear factor kappa B by phosphorylated translation initiation factor 2. *Mol. Cell. Biol.* **24**, 10161–10168 (2004).
17. R. C. Wek, H. Y. Jiang, T. G. Anthony, Coping with stress: eIF2 kinases and translational control. *Biochem. Soc. Trans.* **34**, 7–11 (2006).
18. J. Gil, J. Alcamí, M. Esteban, Activation of NF-kappa B by the dsRNA-dependent protein kinase, PKR involves the I kappa B kinase complex. *Oncogene* **19**, 1369–1378 (2000).
19. J. Gil *et al.*, TRAF family proteins link PKR with NF-kappa B activation. *Mol. Cell. Biol.* **24**, 4502–4512 (2004).
20. C. S. McAllister, N. Taghavi, C. E. Samuel, Protein kinase PKR amplification of interferon β induction occurs through initiation factor eIF-2α-mediated translational control. *J. Biol. Chem.* **287**, 36384–36392 (2012).
21. M. S. Hayden, A. P. West, S. Ghosh, NF-kappaB and the immune response. *Oncogene* **25**, 6758–6780 (2006).
22. T. Liu, L. Zhang, D. Joo, S. C. Sun, NF-κB signaling in inflammation. *Signal Transduct. Target. Ther.* **2**, 17023 (2017).
23. H. Zhang, S. C. Sun, NF-κB in inflammation and renal diseases. *Cell Biosci.* **5**, 63 (2015).
24. E. Zandi, D. M. Rothwarf, M. Delhase, M. Hayakawa, M. Karin, The IkappaB kinase complex (IKK) contains two kinase subunits, IKKalpha and IKKbeta, necessary for IkappaB phosphorylation and NF-kappaB activation. *Cell* **91**, 243–252 (1997).
25. H. L. Pahl, Activators and target genes of Rel/NF-kappaB transcription factors. *Oncogene* **18**, 6853–6866 (1999).
26. A. Hoffmann, A. Levchenko, M. L. Scott, D. Baltimore, The IkappaB-NF-kappaB signaling module: Temporal control and selective gene activation. *Science* **298**, 1241–1245 (2002).
27. V. F. Shih *et al.*, Kinetic control of negative feedback regulators of NF-kappaB/RelA determines their pathogen- and cytokine-receptor signaling specificity. *Proc. Natl. Acad. Sci. U.S.A.* **106**, 9619–9624 (2009).
28. S. Rothenburg, E. J. Seo, J. S. Gibbs, T. E. Dever, K. Dittmar, Rapid evolution of protein kinase PKR alters sensitivity to viral inhibitors. *Nat. Struct. Mol. Biol.* **16**, 63–70 (2009).
29. J. Nejepinska, R. Malik, S. Wagner, P. Svoboda, Reporters transiently transfected into mammalian cells are highly sensitive to translational repression induced by dsRNA expression. *PLoS One* **9**, e87517 (2014).
30. C. Park *et al.*, Orthopoxvirus K3 orthologs show virus- and host-specific inhibition of the antiviral protein kinase PKR. *PLoS Pathog.* **17**, e1009183 (2021).
31. S. C. Sun, P. A. Ganchi, D. W. Ballard, W. C. Greene, NF-kappa B controls expression of inhibitor I kappa B alpha: Evidence for an inducible autoregulatory pathway. *Science* **259**, 1912–1915 (1993).
32. K. Brown, S. Park, T. Kanno, G. Franzoso, U. Siebenlist, Mutual regulation of the transcriptional activator NF-kappa B and its inhibitor, I kappa B-alpha. *Proc. Natl. Acad. Sci. U.S.A.* **90**, 2532–2536 (1993).
33. T. R. Frey *et al.*, Ectromelia virus accumulates less double-stranded RNA compared to vaccinia virus in BS-C-1 cells. *Virology* **509**, 98–111 (2017).
34. S. W. Liu, G. C. Katsafanas, R. Liu, L. S. Wyatt, B. Moss, Poxvirus decapping enzymes enhance virulence by preventing the accumulation of dsRNA and the induction of innate antiviral responses. *Cell Host Microbe* **17**, 320–331 (2015).

35. T. A. Ramelot *et al.*, Myxoma virus immunomodulatory protein M156R is a structural mimic of eukaryotic translation initiation factor eIF2alpha. *J. Mol. Biol.* **322**, 943–954 (2002).
36. A. C. Dar, T. E. Dever, F. Sicheri, Higher-order substrate recognition of eIF2alpha by the RNA-dependent protein kinase PKR. *Cell* **122**, 887–900 (2005).
37. A. Kumar, J. Haque, J. Lacoste, J. Hiscott, B. R. Williams, Double-stranded RNA-dependent protein kinase activates transcription factor NF-kappa B by phosphorylating I kappa B. *Proc. Natl. Acad. Sci. U.S.A.* **91**, 6288–6292 (1994).
38. A. E. Koromilas *et al.*, The interferon-inducible protein kinase PKR modulates the transcriptional activation of immunoglobulin kappa gene. *J. Biol. Chem.* **270**, 25426–25434 (1995).
39. M. Zamanian-Daryoush, T. H. Mogensen, J. A. DiDonato, B. R. Williams, NF-kappaB activation by double-stranded-RNA-activated protein kinase (PKR) is mediated through NF-kappaB-inducing kinase and IkappaB kinase. *Mol. Cell. Biol.* **20**, 1278–1290 (2000).
40. M. C. Bonnet, R. Weil, E. Dam, A. G. Hovanessian, E. F. Meurs, PKR stimulates NF-kappaB irrespective of its kinase function by interacting with the IkappaB kinase complex. *Mol. Cell. Biol.* **20**, 4532–4542 (2000).
41. J. Gil, J. Rullas, M. A. García, J. Alcamí, M. Esteban, The catalytic activity of dsRNA-dependent protein kinase, PKR, is required for NF-kappaB activation. *Oncogene* **20**, 385–394 (2001).
42. H. Y. Jiang *et al.*, Phosphorylation of the alpha subunit of eukaryotic initiation factor 2 is required for activation of NF-kappaB in response to diverse cellular stresses. *Mol. Cell. Biol.* **23**, 5651–5663 (2003).
43. H. Y. Jiang, R. C. Wek, GCN2 phosphorylation of eIF2alpha activates NF-kappaB in response to UV irradiation. *Biochem. J.* **385**, 371–380 (2005).
44. J. J. Dennehy, Evolutionary ecology of virus emergence. *Ann. N. Y. Acad. Sci.* **1389**, 124–146 (2017).
45. F. Fenner, G. M. Woodroofe, The pathogenesis of infectious myxomatosis: The mechanism of infection and the immunological response in the European rabbit (*Oryctolagus cuniculus*). *Br. J. Exp. Pathol.* **34**, 400–411 (1953).
46. M. P. Bevilacqua, M. A. Gimbrone Jr., Inducible endothelial functions in inflammation and coagulation. *Semin. Thromb. Hemost.* **13**, 425–433 (1987).
47. M. Leick, V. Azcutia, G. Newton, F. W. Luscinskas, Leukocyte recruitment in inflammation: Basic concepts and new mechanistic insights based on new models and microscopic imaging technologies. *Cell Tissue Res.* **355**, 647–656 (2014).
48. G. L. Smith, C. Talbot-Cooper, Y. Lu, How does vaccinia virus interfere with interferon? *Adv. Virus Res.* **100**, 355–378 (2018).
49. H. Yu, R. C. Bruneau, G. Brennan, S. Rothenburg, Battle royale: Innate recognition of poxviruses and viral immune evasion. *Biomedicines* **9**, 765 (2021).
50. Y. Zhou *et al.*, Orf virus ORF120 protein positively regulates the NF-κB pathway by interacting with G3BP1. *J. Virol.* **95**, e0015321 (2021).
51. K. S. Carpentier, N. M. Esparo, S. J. Child, A. P. Geballe, A single amino acid dictates protein kinase R susceptibility to unrelated viral antagonists. *PLoS Pathog.* **12**, e1005966 (2016).
52. S. Rothenburg, V. G. Chinchar, T. E. Dever, Characterization of a ranavirus inhibitor of the antiviral protein kinase PKR. *BMC Microbiol.* **11**, 56 (2011).
53. C. Peng, "Host species-specific interactions of protein kinase R and poxvirus pseudosubstrate inhibitors," PhD dissertation, Kansas State University, Manhattan, KS (2016).